

# Synthesis and structures of $\text{Ir}_3\text{Mg}_{13-x}\text{In}_x$ ( $x = 2.37$ and $3.36$ )

Viktor Hlukhyy and Rainer Pöttgen\*

*Institut für Anorganische und Analytische Chemie, Universität Münster, Wilhelm-Klemm-Straße 8, D-48149 Münster, Germany*

Received 23 October 2003; received in revised form 8 December 2003; accepted 14 December 2003

## Abstract

New intermetallic compounds  $\text{Ir}_3\text{Mg}_{13-x}\text{In}_x$  ( $x = 2.37$  and  $3.36$ ) were synthesized by induction melting of the elements in glassy carbon or tantalum crucibles in a water-cooled sample chamber. Both compounds were investigated by X-ray powder diffraction and the structures have been refined on the basis of single-crystal diffractometer data:  $R\bar{3}c$ ,  $a = 1606.2(1)$ ,  $c = 843.37(7)$  pm,  $wR^2 = 0.0689$ , 928  $F^2$  values, 33 variables for  $x = 2.37$  and  $a = 1608.1(1)$ ,  $c = 843.32(6)$  pm,  $wR^2 = 0.0366$ , 929  $F^2$  values, 33 variables for  $x = 3.36$ . The complex crystal structure has only one iridium site with coordination number CN=11. The four crystallographically independent magnesium sites show all mixed Mg/In occupancy with between 3% and 41% indium. The structure can be described by an intergrowth of CN11, 14, 15, 14, and 12 polyhedra of Ir, Mg1/In1, Mg2/In2, Mg3/In3, and Mg4/In4, respectively.

© 2004 Elsevier Inc. All rights reserved.

**Keywords:** Intermetallic compounds; Crystal structure; Indium

## 1. Introduction

Stannides and indides in the ternary systems (Ca, Sr, Ba)– $T$ –In(Sn) ( $T$  = late transition metal) have a general structural motif. The transition metal and indium(tin) atoms build a two- or three-dimensional  $[T_x\text{In}_y]$  or  $[T_x\text{Sn}_y]$  polyanion, where the Ca, Sr, or Ba atoms separate the polyanionic layers or fill channels within the polyanions [1–4, and references therein]. The situation is different when magnesium is used as alkaline earth metal component. Some compounds with a crystal chemistry similar to the higher homologues exist, i.e.,  $\text{MgCuSn}$  and  $\text{MgCu}_4\text{Sn}$  [5],  $\text{MgNi}_2\text{Sn}$  [6],  $\text{MgPtSn}$  and  $\text{MgAuSn}$  [7],  $\text{MgRuSn}_4$  [8],  $\text{MgCu}_4\text{In}$  [9], and  $\text{MgNi}_2\text{In}$  [10]. On the other hand, we observed significant Mg/Sn and Mg/In mixing for various binary transition metal stannides and indides. The stannides  $\text{Ru}_3\text{Sn}_7$  and  $\text{Ir}_3\text{Sn}_7$  form solid solutions  $\text{Mg}_x\text{Rh}_3\text{Sn}_{7-x}$  ( $x = 0–1.55$ ) [8] and  $\text{Mg}_x\text{Ir}_3\text{Sn}_{7-x}$  ( $x = 0–1.67$ ) [11]. Similar substitutions occur for  $\text{IrIn}_3$ . Up to  $x = 0.73$  the compounds  $\text{IrIn}_{3-x}\text{Mg}_x$  crystallize with the tetragonal  $\text{FeGa}_3$  type structure. With increasing magnesium content, a switch in the structure type is observed.  $\text{Mg}_{0.92}\text{In}_{2.08}\text{Ir}$  adopts the  $\text{Fe}_3\text{C}$  structure (cementite type) [12]. With lower

indium content the solid solution  $\text{IrIn}_{2-x}\text{Mg}_x$  for  $\text{IrIn}_2$  occurs [13]. Furthermore also the binary magnesium–transition metal compounds show Mg/In mixing as is realized for the  $\text{Cu}_3\text{P}$  type solid solution  $\text{Mg}_{3-x}\text{In}_x\text{Ir}$  for  $\text{Mg}_3\text{Ir}$  [13].

A third group of intermetallics in the ternary systems magnesium–transition metal–indium does not derive from binary compounds. Although one observes significant Mg/In mixing, such indides adopt their own structure type, however, also with extended homogeneity ranges. Herein, we report on the synthesis and structure refinements of the indides  $\text{Ir}_3\text{Mg}_{13-x}\text{In}_x$  with  $x = 2.37$  and  $3.36$ .

## 2. Experimental

### 2.1. Synthesis

Starting materials for the preparation of the  $\text{Ir}_3\text{Mg}_{13-x}\text{In}_x$  ( $x = 2.37$  and  $3.36$ ) samples were a magnesium rod (Johnson Matthey,  $\varnothing$  16 mm, >99.5%), iridium powder (Degussa-Hüls, 200 mesh, >99.9%), and indium tear drops (Johnson Matthey, 99.9%). Pieces of the magnesium rod (the surface of the rod was first cut on a turning lathe in order to remove

\*Corresponding author. Fax: +49-251-83-36002.

E-mail address: [pottgen@uni-muenster.de](mailto:pottgen@uni-muenster.de) (R. Pöttgen).

surface impurities), cold-pressed pellets of iridium ( $\varnothing$  6 mm), and indium tear drops were weighed in the atomic ratios Mg<sub>65</sub>:Ir<sub>25</sub>:In<sub>10</sub> (sample 1) and Mg<sub>65</sub>:Ir<sub>18</sub>:In<sub>17</sub> (sample 2). The mixture for sample 1 was placed in a glassy carbon crucible (SIGRADUR<sup>®</sup> G, type GAZ006), while the Mg<sub>65</sub>:Ir<sub>18</sub>:In<sub>17</sub> sample was sealed in a tantalum tube [14]. Both crucibles were placed in a water-cooled sample chamber [15] of an induction furnace (Hüttinger Elektronik, Freiburg, Typ TIG 1.5/300). The mixtures of the elements were first heated under flowing argon up to ca. 1200 K. The argon was purified over silica gel, molecular sieves, and titanium sponge (900 K). The reaction between the elements was visible through a slight heat flash. After the melting procedure the samples were cooled within 1 h to ca. 700 K and finally quenched by switching off the furnace. The light gray samples could easily be separated from the glassy carbon or tantalum crucible. No reactions whatsoever of the samples with the crucible material could be detected. A part of sample 1 was subsequently annealed for 3 months at 670 K in an evacuated silica ampoule. All samples are stable in moist air as compact buttons as well as fine-grained powders. Single crystals exhibit metallic luster.

## 2.2. X-ray diffraction

The polycrystalline products have been characterized through their Guinier powder pattern. The Guinier

camera was equipped with an image plate system (Fujifilm, Basread-1800) and monochromated CuK $\alpha$ <sub>1</sub> radiation.  $\alpha$ -quartz ( $a = 491.30$ ,  $c = 540.46$  pm) was used as an internal standard. The hexagonal lattice parameters (Table 1) were obtained from least-squares fits of the powder data. The correct indexing of the patterns was ensured through intensity calculations [16] taking the atomic positions from the structure refinements. The lattice parameters determined from the powders and the single crystals agreed well. For sample 1 the refined lattice parameters of the annealed part (670 K) agreed within one standard deviation with those derived from the induction melted part. For all samples, the X-ray powder patterns showed very weak additional reflections. According to metallographic analyses, these most likely result from further unknown ternary Mg–Ir–In phases.

Small, irregularly shaped single crystals of the two inductively melted samples and the one annealed at 670 K were obtained by mechanical fragmentation. These crystals were first examined by use of a Buerger camera equipped with an image plate system (Fujifilm BAS-1800) in order to establish suitability for intensity data collection.

Single-crystal intensity data were collected at room temperature by use of a Stoe IPDS II image plate diffractometer with monochromatized MoK $\alpha$  radiation in oscillation mode. All relevant details concerning the data collections are listed in Table 1. Since the

Table 1  
Crystal data and structure refinements for Ir<sub>3</sub>Mg<sub>13-x</sub>In<sub>x</sub> with  $x = 2.37$  and  $3.36$  (space group  $R\bar{3}c$ ,  $Z = 6$ )

Empirical formula	Ir <sub>3</sub> Mg <sub>10.63(5)</sub> In <sub>2.37(5)</sub>	Ir <sub>3</sub> Mg <sub>9.64(5)</sub> In <sub>3.36(5)</sub>
Molar mass (g/mol)	1107.14	1196.74
Unit-cell dimensions (crystal data)	$a = 1606.2(1)$ pm $c = 843.37(7)$ pm $V = 1.8843$ nm <sup>3</sup>	$a = 1608.1(1)$ pm $c = 843.32(6)$ pm $V = 1.8864$ nm <sup>3</sup>
Calculated density (g/cm <sup>3</sup> )	5.85	6.32
Crystal size ( $\mu\text{m}^3$ )	$12 \times 18 \times 150$	$25 \times 25 \times 140$
Detector distance	60 mm	60 mm
Exposure time	10 min	18 min
$\omega$ range; increment	0–180°; 1.0°	0–180°; 1.0°
Integr. param. A, B, EMS	13.0; 3.0; 0.028	14.0; 4.0; 0.012
Transm. ratio (max/min)	2.29	3.14
Abs. coefficient (mm <sup>-1</sup> )	36.4	38.1
$F(000)$	2848	3068
$\theta$ range for data collection	4–35°	4–35°
Range in $hkl$	$\pm 25$ , $\pm 25$ , $-13 < l < 11$	$\pm 25$ , $\pm 25$ , $-11 < l < 13$
Total no. of reflections	8990	9194
Independent reflections	928 ( $R_{\text{int}} = 0.0986$ )	929 ( $R_{\text{int}} = 0.0403$ )
Reflections with $I > 2\sigma(I)$	834 ( $R_{\text{sigma}} = 0.0404$ )	856 ( $R_{\text{sigma}} = 0.0167$ )
Data/parameters	928/33	929/33
Goodness-of-fit on $F^2$	1.193	1.095
Final $R$ indices [ $I > 2\sigma(I)$ ]	$R_1 = 0.0288$ $wR_2 = 0.0666$	$R_1 = 0.0180$ $wR_2 = 0.0357$
$R$ indices (all data)	$R_1 = 0.0350$ $wR_2 = 0.0689$	$R_1 = 0.0219$ $wR_2 = 0.0366$
Extinction coefficient	0.00057(4)	0.00030(2)
Largest diff. peak and hole	1.94 and $-1.88$ e/Å <sup>3</sup>	0.97 and $-0.99$ e/Å <sup>3</sup>

Table 2

Atomic coordinates and equivalent isotropic displacement parameters ( $\text{pm}^2$ ) for  $\text{Ir}_3\text{Mg}_{10.63}\text{In}_{2.37}$  and  $\text{Ir}_3\text{Mg}_{9.64}\text{In}_{3.36}$  (space group  $R\bar{3}c$ , hexagonal setting)

Atom	Wyckoff position	Occup. (%)	$x$	$y$	$z$	$U_{\text{eq}}$
$\text{Ir}_3\text{Mg}_{10.63}\text{In}_{2.37}$						
Ir	18e	100	0.17166(2)	0	1/4	95(1)
Mg1/In1	18e	67.5(5)/32.5(5)	0.6366(1)	0	1/4	172(4)
Mg2/In2	6a	79.8(9)/20.2(9)	0	0	1/4	213(10)
Mg3/In3	36f	81.6(4)/18.4(4)	0.4918(1)	0.1874(1)	0.9145(1)	235(5)
Mg4/In4	18d	96.8(5)/3.2(5)	1/2	0	0	214(10)
$\text{Ir}_3\text{Mg}_{9.64}\text{In}_{3.36}$						
Ir	18e	100	0.17145(1)	0	1/4	92(1)
Mg1/In1	18e	58.6(3)/41.4(3)	0.63714(5)	0	1/4	159(2)
Mg2/In2	6a	73.6(5)/26.4(5)	0	0	1/4	194(5)
Mg3/In3	36f	71.3(2)/28.7(2)	0.49123(6)	0.18675(5)	0.91473(7)	221(2)
Mg4/In4	18d	95.6(3)/4.4(3)	1/2	0	0	197(6)

$U_{\text{eq}}$  is defined as one-third of the trace of the orthogonalized  $U_{ij}$  tensor.

refinement results of crystals 1 (induction melted) and 2 (annealed at 670 K for 3 months) of sample 1 are almost identical, only the data of crystal 1 are reported here.

### 2.3. Scanning electron microscopy

The compact samples and the single crystals investigated on the imaging plate diffractometer have been analyzed by EDX measurements using a LEICA 420 I scanning electron microscope with MgO, iridium, and indium arsenide as standards. No impurity elements were detected. For the analyses of the bulk samples, irregularly shaped pieces were embedded in a metacrylate matrix, polished and then examined in the scanning electron microscope in backscattering mode. The analyses of the bulk sample 1 and a single crystal of that sample revealed a composition  $63 \pm 2$  at% Mg:  $21 \pm 2$  at% Ir:  $16 \pm 2$  at% In, close to the refined composition  $66 \pm 1$  at% Mg:  $19 \pm 1$  at% Ir:  $15 \pm 1$  at% In. The EDX data and the refined X-ray data of sample 2 were  $58 \pm 2$  at% Mg:  $20 \pm 2$  at% Ir:  $22 \pm 2$  at% In and  $60 \pm 1$  at% Mg:  $19 \pm 1$  at% Ir:  $21 \pm 1$  at% In, respectively.

### 2.4. Structure refinements

Analysis of the diffractometer data sets revealed rhombohedral  $R$  lattices and the extinction conditions were compatible with space groups  $R\bar{3}c$ ,  $R3c$ ,  $R\bar{3}$ , and  $R32$  of which the space group with the highest symmetry  $R\bar{3}c$  was found to be correct during the structure refinements. The starting atomic parameters were deduced from an automatic interpretation of direct methods with SHELXS-97 [17] and they were subsequently refined using SHELXL-97 [18] (full-matrix least-squares on  $F^2$ ) with isotropic atomic displacement parameters for all atoms. Since the EDX analyses revealed a high magnesium content of the investigated

crystals, in the first refinement cycles the four sites 18e, 6a, 36f, and 18d were refined with the scattering factor of magnesium. The isotropic displacement parameters for these sites and the refined occupancy parameters readily indicated a higher scattering power for all four positions. In the subsequent cycles magnesium/indium mixing was allowed leading to the compositions listed in Table 1. In the final refinement these occupancy parameters were refined as a least-squares variable and all sites were refined with anisotropic atomic displacement parameters. The M4 sites show only minor Mg/In mixing. Refinements exclusively with the scattering power of magnesium resulted in 110(2)% and 114(1)% magnesium occupancy for the two data sets, thus clearly reflecting the Mg/In mixing. The final difference Fourier synthesis were flat (Table 1). The compositions obtained from the structure refinements are  $\text{Ir}_3\text{Mg}_{10.63(5)}\text{In}_{2.37(5)}$  and  $\text{Ir}_3\text{Mg}_{9.64(5)}\text{In}_{3.36(5)}$ . The positional parameters and interatomic distances of the refinements are listed in Tables 2 and 3. Listings of the observed and calculated structure factors are available.<sup>1</sup>

## 3. Results and discussion

The compounds  $\text{Ir}_3\text{Mg}_{13-x}\text{In}_x$  ( $x = 2.37$  and  $3.36$ ) crystallize with a new rhombohedral structure type with Pearson code  $hR96$ . Similar to the solid solutions  $\text{IrIn}_{2-x}\text{Mg}_x$  [13] and  $\text{IrIn}_{3-x}\text{Mg}_x$  [12], also for  $\text{Ir}_3\text{Mg}_{13-x}\text{In}_x$  a pronounced homogeneity range exists as is evident from the two different  $x$  values obtained

<sup>1</sup>Details may be obtained from: Fachinformationszentrum Karlsruhe, D-76344 Eggenstein-Leopoldshafen (Germany), by quoting the Registry Nos. CSD-413480 ( $\text{Ir}_3\text{Mg}_{10.63}\text{In}_{2.37}$ ) and CSD-413479 ( $\text{Ir}_3\text{Mg}_{9.64}\text{In}_{3.36}$ ).

Table 3  
Interatomic distances (pm), calculated with the lattice parameters taken from the single-crystal X-ray data of  $\text{Ir}_3\text{Mg}_{9.64}\text{In}_{3.36}$

Ir:	2	M3	272.5	M3:	1	Ir	272.5
	2	M4	273.4		1	Ir	282.5
	1	M2	275.7		1	M3	295.2
	2	M1	278.2		2	M3	295.7
	2	M3	282.5		1	M2	298.0
	2	M3	335.6		1	M1	300.1
M1:	2	Ir	278.2	1	M4	315.9	
	2	M1	292.6	1	M4	317.8	
	2	M3	300.1	1	M4	319.9	
	2	M4	302.9	1	Ir	335.6	
	2	M4	304.9	1	M1	356.6	
	2	M3	356.6	1	M2	382.9	
	2	M3	384.3	1	M1	384.3	
M2:	3	Ir	275.7	M4:	2	Ir	273.4
	6	M3	298.0		2	M1	302.9
	6	M3	382.9		2	M1	304.9
					2	M3	315.9
					2	M3	317.8
					2	M3	319.9

The *M* sites show mixed magnesium/indium occupancy (see Table 2). All distances within the first coordination spheres are listed. Standard deviations are all equal or less than 0.2 pm.

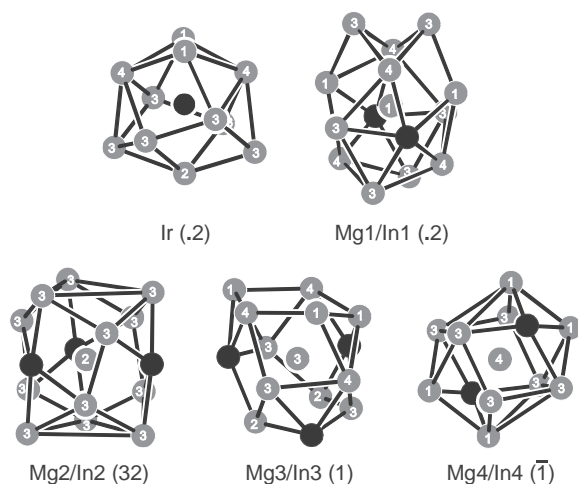


Fig. 1. Coordination polyhedra of the atoms in  $\text{Ir}_3\text{Mg}_{13-x}\text{In}_x$ . The iridium and magnesium/indium atoms are drawn as black and medium gray circles, respectively. The site symmetries are indicated.

from the structure refinements. The limits of the homogeneity range, however, have not been determined. The lattice parameters determined for the powder samples ( $a = 1609.9(3)$ ,  $c = 843.4(1)$  pm for sample 1;  $a = 1606.9(7)$ ,  $c = 844.9(4)$  pm for sample 2) and for the single crystals (Table 1) agreed well. In agreement with the higher indium content for sample 2, the latter shows the higher  $c$  lattice parameter.

The structure contains five crystallographically independent atomic positions. The coordination polyhedra of these sites are shown in Fig. 1. The iridium site is fully occupied and shows coordination number (CN) 11.

The surrounding sites show all mixed magnesium/indium occupancy. The indium substitution on the magnesium positions varies from 3% to 41%. In the following discussion we denote these sites with the letter *M*. The coordination number of the four *M* sites varies from CN 12 to CN 15 with quite irregular coordination polyhedra. This is a direct consequence of the low site symmetries. An overview of the various possible coordination polyhedra in rhombohedral intermetallic compounds was given by Daams and Villars [19].

The  $\text{Ir}_3\text{Mg}_{13-x}\text{In}_x$  structure can be described as an intergrowth of the polyhedra described in Fig. 1. The connectivity pattern of the CN 11 iridium polyhedra is presented in Fig. 2. This drawing shows all atoms of the unit cell. All *M* sites are in the coordination shell of the iridium atoms. The CN 11 iridium polyhedra are condensed via common corners. The three-dimensional network of condensed  $\text{M4Ir}_2\text{M}_{10}$  polyhedra is shown in Fig. 3. These polyhedra can be considered as slightly distorted icosahedra. They share common edges forming a three-dimensional network that leaves channels for the *M2* atoms in the  $00z$ ,  $1/32/3z$  and  $2/31/3z$  directions.

An interesting feature of the structure is shown in Fig. 4. The *M2* atoms within the channels of the *M4* network have coordination number 15 with all iridium and the *M3* atoms in their coordination shell. These polyhedra are condensed in the  $c$  direction via common triangular faces forming one-dimensional rows. These rows form a hexagonal rod packing and they are embedded in a matrix of *M* atoms.

The Ir–*M* distances range from 273 to 283 pm. They compare well with the sum of the covalent radii of 262 pm (Ir + Mg) and 276 pm (Ir + In) [20], indicating strong Ir–*M* interactions. The two longer Ir–*M* distances at 336 pm still belong to the coordination sphere of

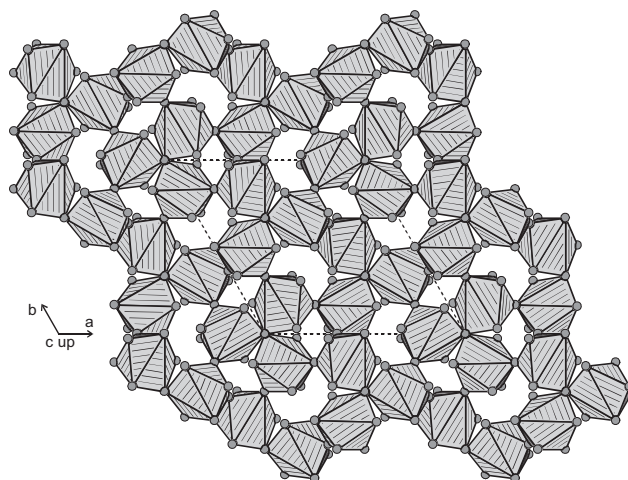


Fig. 2. Projection of the  $\text{Ir}_3\text{Mg}_{13-x}\text{In}_x$  structure along the  $c$ -axis. The magnesium/indium atoms are drawn as medium gray circles. The coordination number 11 polyhedra around the iridium atoms are emphasized.



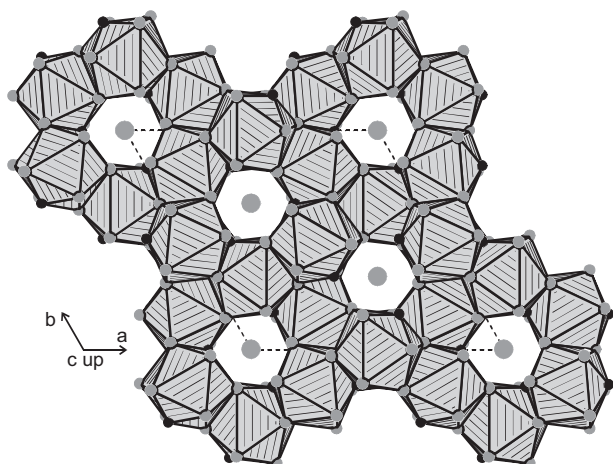


Fig. 3. Projection of the  $\text{Ir}_3\text{Mg}_{13-x}\text{In}_x$  structure along the  $c$ -axis. The iridium and magnesium/indium atoms are drawn as black and medium gray circles, respectively. The coordination number 12 polyhedra around the  $\text{Mg}_4/\text{In}_4$  atoms are emphasized. The  $\text{Mg}_2/\text{In}_2$  atoms are located in the channels formed by this network.

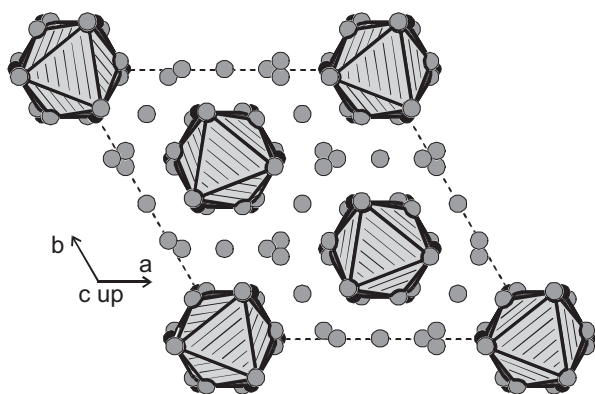


Fig. 4. Projection of the  $\text{Ir}_3\text{Mg}_{13-x}\text{In}_x$  structure along the  $c$ -axis. The iridium and magnesium/indium atoms are drawn as black and medium gray circles, respectively. The coordination number 15 polyhedra around the  $\text{Mg}_2/\text{In}_2$  atoms are emphasized. They are embedded in a matrix of  $\text{Mg}/\text{In}$  atoms.

iridium, resulting in a spherical polyhedron for the iridium site. Similar ranges have recently been observed for the solid solution  $\text{IrIn}_{3-x}\text{In}_x$  (265–277 pm for the  $\text{FeGa}_3$  type modification and 271–283 pm for the  $\text{Fe}_3\text{C}$  type modification) [12],  $\text{IrIn}_{2-x}\text{Mg}_x$  (271–284 pm) [13], and  $\text{Mg}_{3-x}\text{In}_x\text{Ir}$  (263–331 pm) [13]. The various  $M-M$  distances cover the large range from 293 to 384 pm. Every  $M$  atom, however, has between 6 and 10 nearest  $M$  neighbors at  $M-M$  distances smaller or equal to 320 pm. These shorter  $M-M$  distances compare well with the average  $\text{Mg}-\text{Mg}$  distance of 320 pm in *hcp* magnesium [21], while the longer ones are close to the distances in tetragonal body-centered indium [21], where each indium atom has four nearest indium neighbors at 325 pm and eight further neighbors at 338 pm.

In summary, we observe a complicated network of interpenetrating polyhedra for the intermetallics

$\text{Ir}_3\text{Mg}_{13-x}\text{In}_x$  ( $x = 2.37$  and  $3.36$ ). The crystal chemistry of these compounds differs significantly from that of the  $(\text{Ca}, \text{Sr}, \text{Ba})-T-\text{In}$  intermetallics [1–4, and references therein], where the transition metal and indium atoms build a polyanion, in which the  $(\text{Ca}, \text{Sr}, \text{Ba})$  atoms fill channels or separate polyanionic layers [22,23]. Magnesium does not behave like a typical alkaline earth element in this peculiar family of intermetallics.

## Acknowledgments

We are grateful to Dipl.-Ing. U.Ch. Rodewald for the intensity data collections. This work was financially supported by the Fonds der Chemischen Industrie, the Deutsche Forschungsgemeinschaft, and the Bundesministerium für Bildung, Wissenschaft, Forschung und Technologie.

## References

- [1] R.-D. Hoffmann, D. Kußmann, U.Ch. Rodewald, R. Pöttgen, C. Rosenhahn, B.D. Mosel, *Z. Naturforsch.* 54b (1999) 709.
- [2] R.-D. Hoffmann, R. Pöttgen, *Chem. Eur. J.* 6 (2000) 600.
- [3] R.-D. Hoffmann, D. Kußmann, R. Pöttgen, *Int. J. Inorg. Mater.* 2 (2000) 135.
- [4] R.-D. Hoffmann, R. Pöttgen, *Chem. Eur. J.* 7 (2001) 382.
- [5] K. Osamura, Y. Murakami, *J. Less-Common Met.* 60 (1978) 311.
- [6] P. Rahlfs, *Metallwirtsch. Metallwiss. Metalltech.* 16 (1937) 640.
- [7] U. Eberz, W. Seelentag, H.-U. Schuster, *Z. Naturforsch.* 35b (1980) 1341.
- [8] M. Schlüter, A. Kunst, R. Pöttgen, *Z. Anorg. Allg. Chem.* 628 (2002) 2641.
- [9] M.Y. Teslyuk, P.I. Krypyakevich, *Dopov. Akad. Nauk Ukr. RSR* 8 (1961) 1039.
- [10] V.Ya. Markiv, M.Y. Teslyuk, *Dopov. Akad. Nauk Ukr. RSR* 12 (1962) 1607.
- [11] M. Schlüter, U. Häussermann, B. Heying, R. Pöttgen, *J. Solid State Chem.* 173 (2003) 418.
- [12] V. Hlukhyy, R.-D. Hoffmann, R. Pöttgen, *Z. Anorg. Allg. Chem.* 630 (2004) 68.
- [13] V. Hlukhyy, R.-D. Hoffmann, R. Pöttgen, *Intermetallics*, in press.
- [14] R. Pöttgen, Th. Gulden, A. Simon, *GIT Labor-Fachzeitsch.* 43 (1999) 133.
- [15] D. Kußmann, R.-D. Hoffmann, R. Pöttgen, *Z. Anorg. Allg. Chem.* 624 (1998) 1727.
- [16] K. Yvon, W. Jeitschko, E. Parthé, *J. Appl. Crystallogr.* 10 (1977) 73.
- [17] G.M. Sheldrick, *SHELXS-97, Program for the Determination of Crystal Structures*, University of Göttingen, 1997.
- [18] G.M. Sheldrick, *SHELXL-97, Program for Crystal Structure Refinement*, University of Göttingen, 1997.
- [19] J.L.C. Daams, P. Villars, *J. Alloys Compd.* 197 (1993) 243.
- [20] J. Emsley, *The Elements*, Oxford University Press, Oxford, 1999.
- [21] J. Donohue, *The Structures of the Elements*, Wiley, New York, 1974.
- [22] R.-D. Hoffmann, R. Pöttgen, *Chem. Eur. J.* 7 (2001) 382.
- [23] R.-D. Hoffmann, R. Pöttgen, *Z. Anorg. Allg. Chem.* 626 (2000) 29.